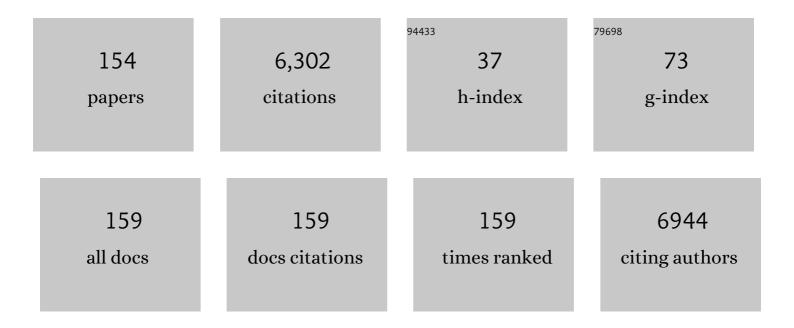
List of Publications by Year in descending order

Source: https://exaly.com/author-pdf/7075272/publications.pdf Version: 2024-02-01



Ρινιζκιιν Υλν

#	Article	IF	CITATIONS
1	Low-Dose CT Image Denoising Using a Generative Adversarial Network With Wasserstein Distance and Perceptual Loss. IEEE Transactions on Medical Imaging, 2018, 37, 1348-1357.	8.9	983
2	Magnetic Resonance Imaging/Ultrasound Fusion Guided Prostate Biopsy Improves Cancer Detection Following Transrectal Ultrasound Biopsy and Correlates With Multiparametric Magnetic Resonance Imaging. Journal of Urology, 2011, 186, 1281-1285.	0.4	408
3	Deep learning in medical image registration: a survey. Machine Vision and Applications, 2020, 31, 1.	2.7	343
4	Manifold Regularized Sparse NMF for Hyperspectral Unmixing. IEEE Transactions on Geoscience and Remote Sensing, 2013, 51, 2815-2826.	6.3	322
5	Saliency Detection by Multiple-Instance Learning. IEEE Transactions on Cybernetics, 2013, 43, 660-672.	9.5	163
6	Automatic Segmentation of High-Throughput RNAi Fluorescent Cellular Images. IEEE Transactions on Information Technology in Biomedicine, 2008, 12, 109-117.	3.2	137
7	Boundary-Weighted Domain Adaptive Neural Network for Prostate MR Image Segmentation. IEEE Transactions on Medical Imaging, 2020, 39, 753-763.	8.9	135
8	Deeply-supervised CNN for prostate segmentation. , 2017, , .		117
9	D'Amico Risk Stratification Correlates With Degree of Suspicion of Prostate Cancer on Multiparametric Magnetic Resonance Imaging. Journal of Urology, 2011, 185, 815-820.	0.4	113
10	Learning deep similarity metric for 3D MR–TRUS image registration. International Journal of Computer Assisted Radiology and Surgery, 2019, 14, 417-425.	2.8	101
11	Multi-Organ Segmentation Over Partially Labeled Datasets With Multi-Scale Feature Abstraction. IEEE Transactions on Medical Imaging, 2020, 39, 3619-3629.	8.9	101
12	Discrete Deformable Model Guided by Partial Active Shape Model for TRUS Image Segmentation. IEEE Transactions on Biomedical Engineering, 2010, 57, 1158-1166.	4.2	100
13	Fast fit-free analysis of fluorescence lifetime imaging via deep learning. Proceedings of the National Academy of Sciences of the United States of America, 2019, 116, 24019-24030.	7.1	100
14	Single-image super-resolution via local learning. International Journal of Machine Learning and Cybernetics, 2011, 2, 15-23.	3.6	95
15	Linear SVM classification using boosting HOG features for vehicle detection in low-altitude airborne videos. , 2011, , .		87
16	Alternatively Constrained Dictionary Learning For Image Superresolution. IEEE Transactions on Cybernetics, 2014, 44, 366-377.	9.5	81
17	MR Image Super-Resolution via Wide Residual Networks With Fixed Skip Connection. IEEE Journal of Biomedical and Health Informatics, 2019, 23, 1129-1140.	6.3	81
18	Greedy regression in sparse coding space for single-image super-resolution. Journal of Visual Communication and Image Representation, 2013, 24, 148-159.	2.8	79

Ρινςκύν Υάν

#	Article	IF	CITATIONS
19	Segmentation of volumetric MRA images by using capillary active contour. Medical Image Analysis, 2006, 10, 317-329.	11.6	75
20	Vehicle Detection and Motion Analysis in Low-Altitude Airborne Video Under Urban Environment. IEEE Transactions on Circuits and Systems for Video Technology, 2011, 21, 1522-1533.	8.3	75
21	Visual Saliency by Selective Contrast. IEEE Transactions on Circuits and Systems for Video Technology, 2013, 23, 1150-1155.	8.3	74
22	Image Super-Resolution Via Double Sparsity Regularized Manifold Learning. IEEE Transactions on Circuits and Systems for Video Technology, 2013, 23, 2022-2033.	8.3	71
23	Robust visual tracking with discriminative sparse learning. Pattern Recognition, 2013, 46, 1762-1771.	8.1	70
24	Multi-spectral saliency detection. Pattern Recognition Letters, 2013, 34, 34-41.	4.2	70
25	Net-FLICS: fast quantitative wide-field fluorescence lifetime imaging with compressed sensing – a deep learning approach. Light: Science and Applications, 2019, 8, 26.	16.6	64
26	Adaptively Learning Local Shape Statistics for Prostate Segmentation in Ultrasound. IEEE Transactions on Biomedical Engineering, 2011, 58, 633-641.	4.2	62
27	3D Model based Object Class Detection in An Arbitrary View. , 2007, , .		61
28	Deep Recurrent Neural Networks for Prostate Cancer Detection: Analysis of Temporal Enhanced Ultrasound. IEEE Transactions on Medical Imaging, 2018, 37, 2695-2703.	8.9	57
29	Integrative analysis for COVID-19 patient outcome prediction. Medical Image Analysis, 2021, 67, 101844.	11.6	57
30	Adversarial Image Registration with Application for MR and TRUS Image Fusion. Lecture Notes in Computer Science, 2018, , 197-204.	1.3	54
31	Changes in prostate cancer detection rate of MRI-TRUS fusion vs systematic biopsy over time: evidence of a learning curve. Prostate Cancer and Prostatic Diseases, 2017, 20, 436-441.	3.9	52
32	A method of rapid quantification of patientâ€specific organ doses for CT using deepâ€learningâ€based multiâ€organ segmentation and GPUâ€accelerated Monte Carlo dose computing. Medical Physics, 2020, 47, 2526-2536.	3.0	49
33	Adaptive Shape Prior Constrained Level Sets for Bladder MR Image Segmentation. IEEE Journal of Biomedical and Health Informatics, 2014, 18, 1707-1716.	6.3	48
34	Ageâ€related changes in prostate zonal volumes as measured by highâ€resolution magnetic resonance imaging (MRI): a crossâ€sectional study in over 500 patients. BJU International, 2012, 110, 1642-1647.	2.5	45
35	Feature Fusion Encoder Decoder Network for Automatic Liver Lesion Segmentation. , 2019, , .		45
36	Transfer learning for pedestrian detection. Neurocomputing, 2013, 100, 51-57.	5.9	44

Ρινςκύν Υάν

#	Article	IF	CITATIONS
37	Selecting Key Poses on Manifold for Pairwise Action Recognition. IEEE Transactions on Industrial Informatics, 2012, 8, 168-177.	11.3	43
38	Deep learning predicts cardiovascular disease risks from lung cancer screening low dose computed tomography. Nature Communications, 2021, 12, 2963.	12.8	43
39	Learning 4D action feature models for arbitrary view action recognition. , 2008, , .		41
40	Vehicle detection and tracking in airborne videos by multi-motion layer analysis. Machine Vision and Applications, 2012, 23, 921-935.	2.7	40
41	Pylon line spatial correlation assisted transmission line detection. IEEE Transactions on Aerospace and Electronic Systems, 2014, 50, 2890-2905.	4.7	38
42	Exploiting Interslice Correlation for MRI Prostate Image Segmentation, from Recursive Neural Networks Aspect. Complexity, 2018, 2018, 1-10.	1.6	37
43	Detection and grading of prostate cancer using temporal enhanced ultrasound: combining deep neural networks and tissue mimicking simulations. International Journal of Computer Assisted Radiology and Surgery, 2017, 12, 1293-1305.	2.8	36
44	Sparse coding for image denoising using spike and slab prior. Neurocomputing, 2013, 106, 12-20.	5.9	35
45	A Homographic Framework for the Fusion of Multi-view Silhouettes. , 2007, , .		34
46	Robust Alternative Minimization for Matrix Completion. IEEE Transactions on Systems, Man, and Cybernetics, 2012, 42, 939-949.	5.0	34
47	Multiparametric magnetic resonance imaging-transrectal ultrasound fusion–assisted biopsy for the diagnosis of local recurrence after radical prostatectomy. Urologic Oncology: Seminars and Original Investigations, 2015, 33, 425.e1-425.e6.	1.6	32
48	Medical Image Segmentation Using Minimal Path Deformable Models With Implicit Shape Priors. IEEE Transactions on Information Technology in Biomedicine, 2006, 10, 677-684.	3.2	31
49	Segmenting Images by Combining Selected Atlases on Manifold. Lecture Notes in Computer Science, 2011, 14, 272-279.	1.3	30
50	The Role of Image Guided Biopsy Targeting in Patients with Atypical Small Acinar Proliferation. Journal of Urology, 2015, 193, 473-478.	0.4	30
51	Sensorless Freehand 3D Ultrasound Reconstruction via Deep Contextual Learning. Lecture Notes in Computer Science, 2020, , 463-472.	1.3	30
52	Motion Compensated Lossy-to-Lossless Compression of 4-D Medical Images Using Integer Wavelet Transforms. IEEE Transactions on Information Technology in Biomedicine, 2005, 9, 132-138.	3.2	29
53	Geometry constrained sparse coding for single image super-resolution. , 2012, , .		29
54	Prostate Segmentation in MR Images Using Discriminant Boundary Features. IEEE Transactions on Biomedical Engineering, 2013, 60, 479-488.	4.2	29

Ρινσκύν Υάν

#	Article	IF	CITATIONS
55	Cross-Modal Attention for MRI and Ultrasound Volume Registration. Lecture Notes in Computer Science, 2021, , 66-75.	1.3	29
56	Shadow-Consistent Semi-Supervised Learning for Prostate Ultrasound Segmentation. IEEE Transactions on Medical Imaging, 2022, 41, 1331-1345.	8.9	28
57	Ego motion guided particle filter for vehicle tracking in airborne videos. Neurocomputing, 2014, 124, 168-177.	5.9	27
58	Object-aware power line detection using color and near-infrared images. IEEE Transactions on Aerospace and Electronic Systems, 2014, 50, 1374-1389.	4.7	27
59	Machine learning in medical imaging. Computerized Medical Imaging and Graphics, 2015, 41, 1-2.	5.8	27
60	Learning Saliency by MRF and Differential Threshold. IEEE Transactions on Cybernetics, 2013, 43, 2032-2043.	9.5	26
61	Transfer learning from RF to B-mode temporal enhanced ultrasound features for prostate cancer detection. International Journal of Computer Assisted Radiology and Surgery, 2017, 12, 1111-1121.	2.8	25
62	Correlation-Based Tracking of Multiple Targets With Hierarchical Layered Structure. IEEE Transactions on Cybernetics, 2018, 48, 90-102.	9.5	24
63	Deep adaptive registration of multi-modal prostate images. Computerized Medical Imaging and Graphics, 2020, 84, 101769.	5.8	24
64	Synergizing medical imaging and radiotherapy with deep learning. Machine Learning: Science and Technology, 2020, 1, 021001.	5.0	24
65	Knowledge-Based Analysis for Mortality Prediction From CT Images. IEEE Journal of Biomedical and Health Informatics, 2020, 24, 457-464.	6.3	23
66	High compression deep learning based single-pixel hyperspectral macroscopic fluorescence lifetime imaging in vivo. Biomedical Optics Express, 2020, 11, 5401.	2.9	23
67	Is Visual Registration Equivalent to Semiautomated Registration in Prostate Biopsy?. BioMed Research International, 2015, 2015, 1-7.	1.9	22
68	Biopsy needle detection in transrectal ultrasound. Computerized Medical Imaging and Graphics, 2011, 35, 653-659.	5.8	21
69	Global structure constrained local shape prior estimation for medical image segmentation. Computer Vision and Image Understanding, 2013, 117, 1017-1026.	4.7	21
70	Association of AI quantified COVID-19 chest CT and patient outcome. International Journal of Computer Assisted Radiology and Surgery, 2021, 16, 435-445.	2.8	21
71	Feature competition and partial sparse shape modeling for cardiac image sequences segmentation. Neurocomputing, 2015, 149, 904-913.	5.9	20
72	Shape prior constrained PSO model for bladder wall MRI segmentation. Neurocomputing, 2018, 294, 19-28.	5.9	20

#	Article	IF	CITATIONS
73	Deep learning-based liver segmentation for fusion-guided intervention. International Journal of Computer Assisted Radiology and Surgery, 2020, 15, 963-972.	2.8	20
74	Deep neural networks for the assessment of surgical skills: A systematic review. Journal of Defense Modeling and Simulation, 2022, 19, 159-171.	1.7	19
75	Spatio–Temporal Regularity Flow (SPREF): Its Estimation and Applications. IEEE Transactions on Circuits and Systems for Video Technology, 2007, 17, 584-589.	8.3	18
76	Label Image Constrained Multiatlas Selection. IEEE Transactions on Cybernetics, 2015, 45, 1158-1168.	9.5	18
77	Deep neural maps for unsupervised visualization of high-grade cancer in prostate biopsies. International Journal of Computer Assisted Radiology and Surgery, 2019, 14, 1009-1016.	2.8	17
78	Functional Brain Imaging Reliably Predicts Bimanual Motor Skill Performance in a Standardized Surgical Task. IEEE Transactions on Biomedical Engineering, 2021, 68, 2058-2066.	4.2	17
79	MRA Image Segmentation with Capillary Active Contour. Lecture Notes in Computer Science, 2005, 8, 51-58.	1.3	17
80	Image registration by normalized mapping. Neurocomputing, 2013, 101, 181-189.	5.9	16
81	Hierarchical incorporation of shape and shape dynamics for flying bird detection. Neurocomputing, 2014, 131, 179-190.	5.9	16
82	Investigation of Physical Phenomena Underlying Temporal-Enhanced Ultrasound as a New Diagnostic Imaging Technique: Theory and Simulations. IEEE Transactions on Ultrasonics, Ferroelectrics, and Frequency Control, 2018, 65, 400-410.	3.0	16
83	Unsupervised Domain Adaptation with Dual-Scheme Fusion Network for Medical Image Segmentation. , 2020, , .		16
84	Robust color correction in stereo vision. , 2011, , .		15
85	Prostate Biopsy for the Interventional Radiologist. Journal of Vascular and Interventional Radiology, 2014, 25, 675-684.	0.5	15
86	PASiam: Predicting Attention Inspired Siamese Network, for Space-Borne Satellite Video Tracking. , 2019, , .		15
87	Decreasing the Surgical Errors by Neurostimulation of Primary Motor Cortex and the Associated Brain Activation via Neuroimaging. Frontiers in Neuroscience, 2021, 15, 651192.	2.8	15
88	Visual Attention Accelerated Vehicle Detection in Low-Altitude Airborne Video of Urban Environment. IEEE Transactions on Circuits and Systems for Video Technology, 2012, 22, 366-378.	8.3	14
89	Machine Learning in Medical Imaging. International Journal of Biomedical Imaging, 2012, 2012, 1-2.	3.9	13
90	A Deep Learning Health Data Analysis Approach: Automatic 3D Prostate MR Segmentation with Densely-Connected Volumetric ConvNets. , 2018, , .		13

Ρινςκών Υάν

#	Article	IF	CITATIONS
91	Polar transform network for prostate ultrasound segmentation with uncertainty estimation. Medical Image Analysis, 2022, 78, 102418.	11.6	13
92	Single-Image Super-Resolution via Sparse Coding Regression. , 2011, , .		12
93	Estimating patient-specific shape prior for medical image segmentation. , 2011, , .		12
94	Confidence guided enhancing brain tumor segmentation in multi-parametric MRI. , 2012, , .		12
95	Modeling Interaction for Segmentation of Neighboring Structures. IEEE Transactions on Information Technology in Biomedicine, 2009, 13, 252-262.	3.2	11
96	SIFT on manifold: An intrinsic description. Neurocomputing, 2013, 113, 227-233.	5.9	11
97	Segmentation of Neighboring Organs in Medical Image with Model Competition. Lecture Notes in Computer Science, 2005, 8, 270-277.	1.3	11
98	Deep learning for biomechanical modeling of facial tissue deformation in orthognathic surgical planning. International Journal of Computer Assisted Radiology and Surgery, 2022, 17, 945-952.	2.8	11
99	Tracking vehicles as groups in airborne videos. Neurocomputing, 2013, 99, 38-45.	5.9	10
100	OASIS: One-pass aligned atlas set for medical image segmentation. Neurocomputing, 2022, 470, 130-138.	5.9	10
101	Deep learning-based motion artifact removal in functional near-infrared spectroscopy. Neurophotonics, 2022, 9, 041406.	3.3	10
102	Local learning-based image super-resolution. , 2011, , .		9
103	Partial sparse shape constrained sector-driven bladder wall segmentation. Machine Vision and Applications, 2015, 26, 593-606.	2.7	9
104	Multi-Task Learning for Registering Images With Large Deformation. IEEE Journal of Biomedical and Health Informatics, 2021, 25, 1624-1633.	6.3	9
105	Prediction of Coronary Calcification and Stenosis: Role of Radiomics From Low-Dose CT. Academic Radiology, 2021, 28, 972-979.	2.5	9
106	Medical Image Segmentation Using Descriptive Image Features. , 2011, , .		9
107	Medical image segmentation with minimal path deformable models. , 0, , .		8
108	Action recognition using spatio-temporal regularity based features. Proceedings of the IEEE International Conference on Acoustics, Speech, and Signal Processing, 2008, , .	1.8	8

#	Article	IF	CITATIONS
109	Toward a real-time system for temporal enhanced ultrasound-guided prostate biopsy. International Journal of Computer Assisted Radiology and Surgery, 2018, 13, 1201-1209.	2.8	8
110	End-to-end Ultrasound Frame to Volume Registration. Lecture Notes in Computer Science, 2021, , 56-65.	1.3	8
111	Optimal search guided by partial active shape model for prostate segmentation in TRUS images. , 2009, ,		7
112	Rapid pedestrian detection in unseen scenes. Neurocomputing, 2011, 74, 3343-3350.	5.9	7
113	Single-image super-resolution based on semi-supervised learning. , 2011, , .		7
114	Local semi-supervised regression for single-image super-resolution. , 2011, , .		7
115	Learning from Noisy Label Statistics: Detecting High Grade Prostate Cancer in Ultrasound Guided Biopsy. Lecture Notes in Computer Science, 2018, , 21-29.	1.3	7
116	Classifying Cancer Grades Using Temporal Ultrasound for Transrectal Prostate Biopsy. Lecture Notes in Computer Science, 2016, , 653-661.	1.3	7
117	Utilizing homotopy for single image superresolution. , 2011, , .		6
118	Coupled Directional Level Set for MR Image Segmentation. , 2012, , .		6
119	Machine learning in medical imaging. Machine Vision and Applications, 2013, 24, 1327-1329.	2.7	6
120	Task-Oriented Low-Dose CT Image Denoising. Lecture Notes in Computer Science, 2021, , 441-450.	1.3	6
121	Incremental Shape Statistics Learning for Prostate Tracking in TRUS. Lecture Notes in Computer Science, 2010, 13, 42-49.	1.3	6
122	On a Sparse Shortcut Topology of Artificial Neural Networks. IEEE Transactions on Artificial Intelligence, 2022, 3, 595-608.	4.7	6
123	Multi-atlas Based Image Selection with Label Image Constraint. , 2012, , .		5
124	Image Denoising via Improved Sparse Coding. , 2011, , .		5
125	Deep compressive macroscopic fluorescence lifetime imaging. , 2018, , .		4
126	Pedestrian detection in unseen scenes by dynamically updating visual words. Neurocomputing, 2013, 119, 232-242.	5.9	3

#	Article	IF	CITATIONS
127	Ultrasound-Based Predication of Prostate Cancer in MRI-guided Biopsy. Lecture Notes in Computer Science, 2014, , 142-150.	1.3	3
128	T <sub>2</sub> Mapping Refined Finite Element Modeling to Predict Knee Osteoarthritis Progression. , 2021, 2021, 4592-4595.		3
129	Segmenting TRUS video sequences using local shape statistics. , 2010, , .		2
130	A novel alternative algorithm for limited angle tomography. , 2011, , .		2
131	Putting images on a manifold for atlas-based image segmentation. , 2011, , .		2
132	Collaborative Kalman filters for vehicle tracking. , 2011, , .		2
133	Monitoring of radiofrequency ablation with shear wave delay mapping. , 2015, , .		2
134	MP20-16 TRAINING AND SKILLS ASSESSMENT FOR FUSION-GUIDED PROSTATE BIOPSY: DEFINING THE LEARNING CURVE. Journal of Urology, 2016, 195, .	0.4	2
135	Tissue mimicking simulations for temporal enhanced ultrasound-based tissue typing. Proceedings of SPIE, 2017, , .	0.8	2
136	Biomedical imaging and analysis through deep learning. , 2021, , 49-74.		2
137	Transducer Adaptive Ultrasound Volume Reconstruction. , 2021, , .		2
138	Finite element modeling with subjectâ€ <b>s</b> pecific mechanical properties to assess knee osteoarthritis initiation and progression. Journal of Orthopaedic Research, 2023, 41, 72-83.	2.3	2
139	Data Augmentation for Training Deep Neural Networks. , 2021, , 151-164.		1
140	fNIRS as a Quantitative tool to Asses and Predict Surgical Skills. , 2019, , .		1
141	A shell and kernel descriptor based joint deep learning model for predicting breast lesion malignancy. , 2019, , .		1
142	Transformed Grid Distance Loss forÂSupervised Image Registration. Lecture Notes in Computer Science, 2022, , 177-181.	1.3	1
143	Segmentation of Neighboring Structures by Modeling Their Interaction. , 0, , .		0
144	Multi-parametric MRI-pathologic correlation of prostate cancer using tracked biopsies. , 2010, , .		0

#	Article	IF	CITATIONS
145	Image denoising via weight regression. , 2011, , .		0
146	Designing and selecting features for MR image segmentation. , 2011, , .		0
147	Putting poses on manifold for action recognition. , 2011, , .		Ο
148	Learning shape statistics for hierarchical 3D medical image segmentation. , 2011, , .		0
149	Target-oriented shape modeling with structure constraint for image segmentation. , 2011, , .		0
150	Local adaptive dictionary based image denoising. , 2011, , .		0
151	Guest Editorial: Special issue on advanced computing for image-guided intervention. Neurocomputing, 2014, 144, 1-2.	5.9	Ο
152	Surface-based registration of liver in ultrasound and CT. Proceedings of SPIE, 2015, , .	0.8	0
153	Cardiovascular Disease Risk Improves COVID-19 Patient Outcome Prediction. Lecture Notes in Computer Science, 2021, , 467-476.	1.3	Ο
154	Division and Fusion: Rethink Convolutional Kernels for 3D Medical Image Segmentation. Lecture Notes in Computer Science, 2020, , 160-169.	1.3	0